Mapping approach to the semiclassical description of nonadiabatic quantum dynamics

Michael Thoss*
Institute of Physical and Theoretical Chemistry, Technical University of Munich, D-85748 Garching, Germany

Gerhard Stock†
Faculty of Physics, University Freiburg, D-79104 Freiburg, Germany

(Received 3 August 1998)

A theoretical formulation is outlined that allows us to extend the semiclassical Van Vleck–Gutzwiller formulation to the description of nonadiabatic quantum dynamics on coupled potential-energy surfaces. In this formulation the problem of a classical treatment of *discrete* quantum degrees of freedom (DoF) such as electronic states is bypassed by transforming the discrete quantum variables to continuous variables. The mapping approach thus consists of two steps: an exact quantum-mechanical transformation of discrete onto continuous DoF (the ''mapping'') and a standard semiclassical treatment of the resulting dynamical problem. Extending previous work [G. Stock and M. Thoss, Phys. Rev. Lett. **78**, 578 (1997)], various possibilities for obtaining a mapping from discrete to continuous DoF are investigated, in particular the Holstein-Primakoff transformation, Schwinger's theory of angular momentum [in *Quantum Theory of Angular Momentum*, edited by L. C. Biedenharn and H. V. Dam (Academic, New York, 1965)], and the spin-coherent-state representation. Although all these representations are exact on the quantum-mechanical level, the accuracy of their semiclassical evaluation is shown to differ considerably. In particular, it is shown that a generalization of Schwinger's theory appears to be the only transformation that provides an exact description of a general *N*-level system within a standard semiclassical evaluation. Exploiting the connection between spin-coherent states and Schwinger's representation for a two-level system, furthermore, a semiclassical initial-value representation of the corresponding spin-coherent-state propagator is derived. Although this propagator represents an approximation, its appealing numerical features make it a promising candidate for the semiclassical description of large molecular systems with many DoF. Adopting various spin-boson-type models (i.e., a two-level system coupled to a single or many DoF), computational studies are presented for Schwinger's and the spin-coherent-state representation, respectively. The performance of the semiclassical approximation in the case of regular and chaotic classical dynamics as well as for multimode electronic relaxation dynamics is discussed in some detail. [S1050-2947(99)01901-0]

PACS number(s): 03.65.Sq, 31.15.Gy, 03.65.Ge

I. INTRODUCTION

The description of quantum-mechanical dynamics employing a semiclassical approach has been an active field of research since the first days of quantum mechanics [1]. Issues raised include the fundamental question of the classical limit of quantum mechanics, the understanding and interpretation of quantum effects through a classical analysis, and the modeling of dynamical processes in complex systems that defy a rigorous quantum-mechanical treatment.

A classical description is well established in cases where both the system under consideration and the observable to be calculated have an obvious classical analog (say the translational-energy distribution after a scattering event). It is less clear, however, how to incorporate discrete quantum-mechanical degrees of freedom (DoF) into a classical theory. For example, consider a two-level system coupled to one or many continuous DoF. Accounting for a large variety of phenomena in chemical and solid-state physics as well as in quantum optics, this model represents one of the best studied problems [2]. Yet, even for this simple system, the classical limit is not completely understood.

A formal solution to the problem can be obtained within a path-integral formulation. The idea is to construct a path integral for the full problem, and subsequently employ a stationary-phase evaluation for the continuous DoF. Adopting this formalism for a description of nonadiabatic scattering, Pechukas showed that the classical particles (i.e., the nuclei) move in a nonlocal force field generated by the quantum particles (i.e., the electrons) [3]. Employing a classical-path-type evaluation of the electronic transition-amplitude, the ''quantum force'' becomes localized in space and time [4,5], thus leading to Stückelberg's theory of curve crossings [6]. In this formulation, nonadiabatic transitions of classical trajectories are described in terms of a connection formula of the Wentzel-Kramers-Brillouin wave functions associated with the two coupled electronic states. The intuitively appealing picture of trajectories hopping between coupled potential-energy surfaces has been adopted by a number of semiclassical [4–10] and quantum-classical [5,11] descriptions. A problem of this approach to the semiclassical description of nonadiabatic dynamics is, however, that in general only the full (and computationally prohibitive) path-integral formulation is ''semiclassically exact'' in the sense that it requires only the basic semiclassical Van Vleck–

*Present address: Department of Chemistry, University of California, Berkeley, CA 94720.
†Electronic address: stock@physik.uni-freiburg.de

Gutzwiller approximation [1] to the quantum propagator. All other formulations appear to involve additional approximations which often are difficult to control.

Some years ago, McCurdy, Meyer, and Miller suggested an alternative way to the semiclassical description of nonadiabatic dynamics [12–16]. Exploiting various quantum-classical analogies including Heisenberg's correspondence principle [12], a classical pseudopotential ansatz [13], as well as the correspondence of spin and classical angular momentum [15], they constructed classical Hamiltonian functions for the full vibronic system, thus treating both electronic and nuclear DoF's on the same dynamical (i.e., classical) footing. The most successful version, sometimes referred to as the ''classical electron-analog'' model [14], is based on a classical-path ansatz of the Hamiltonian function, and has been employed to several test problems including nonadiabatic collision processes [17]. In an extension to existing classical-path formulations which do not account for interference effects of individual classical paths [18–22], the classical electron-analog model suggests a semiclassical treatment of the dynamics within classical *S*-matrix theory [23]. Although the idea of establishing a classical analogon is conceptionally appealing, the approach is not completely satisfying from a theoretical point of view. Starting out with an approximate classical (rather than an exact quantum-mechanical) formulation, there are two interrelated problems: (i) The formulations are not unique, i.e., various analogies result in different classical models. Furthermore, the formulations do not determine the boundary (or initial) conditions of the semiclassical propagator. (ii) The nature of the approximations involved is difficult to specify. For example, none of the models [12–16] are semiclassically exact, but give approximate results even for a two-level system [14].

Recently we have proposed a ''mapping approach'' to the semiclassical description of nonadiabatic dynamics [24]. In this formulation the problem of a classical treatment of discrete quantum DoF is bypassed by transforming the discrete quantum variables to continuous variables. Based on Schwinger's theory of angular momentum [25], the mapping of discrete DoF onto continuous DoF is achieved through the representation of spin operators by boson operators. To illustrate the concept, consider a molecular system comprising N electronic states and M vibrational modes: The basic idea is to (i) map the N discrete DoF onto N continuous DoF and (ii) solve the resulting dynamical problem of $N+M$ continuous DoF employing standard semiclassical methodology. Since the mapping is quantum mechanically exact, the approach allows us—without any further approximations—to extend well-established techniques of classical trajectory calculations to nonadiabatic problems on coupled potential-energy surfaces.

As both electronic and nuclear DoF are formally treated by classical mechanics, the classical limit of the mapping formulation is in the same spirit as the models of McCurdy, Meyer, and Miller. In particular, a requantized version of the classical electron-analog model recently introduced by Sun and Miller [26] is equivalent to the semiclassical limit of the mapping proposed in Ref. [24]. However, since the mapping approach establishes an equivalence of discrete and continuous DoF *on a quantum-mechanical level*, this approach is free from the problems associated with these models. In particular, (i) the mapping unambiguously defines the Hamiltonian as well as the boundary (or initial) conditions of the semiclassical propagator, and (ii) the approach is semiclassical exact since no additional assumption except for the standard semiclassical approximation is needed. The *quasiclassical* limit (i.e., without semiclassical phases) of the mapping approach and its relation to the classical electron-analog models [12–16] as well as to other classical-path formulations [18–22] have been discussed in Ref. [27].

Bosonization techniques such as Schwinger's theory of angular momentum [25] and the Holstein-Primakoff transformation [28] are well known, and have been applied in various fields including nuclear physics [29], solid-state physics [30,31], and quantum optics [32]. On a quantum-mechanical level, all these representations are exact, thus resulting in a completely equivalent formulation. This is no longer true, however, if the transformed problem is subsequently treated within a semiclassical framework. Depending on the transformation under consideration, the validity and accuracy of the semiclassical approximation may differ considerably. Since the very concept of the mapping approach is to use these transformations as a starting point for a semiclassical treatment of nonadiabatic quantum dynamics, it is essential to investigate the classical limit of various bosonization techniques.

An alternative concept to obtain a continuous description of discrete quantum variables is based on the coherent-state representation of the quantum system under consideration [33,34]. In particular, the spin-coherent-state path integral has been used to investigate the semiclassical description of spin systems [35–37]. At a first sight, the usage of spin-coherent states and the mapping approach appear to be quite different concepts. However, there exists a close connection between these approaches which is discussed in this work. In particular, we use the mapping method to derive a semiclassical spin-coherent-state propagator. It is shown that this propagator can be considered as a generalization of the work by Suzuki [38].

The outline of the paper is as follows. Section II briefly reviews existing mapping formalisms for a spin system and for the more general case of an N-level system. Furthermore the connection of the mappings to the formalism of second quantization is discussed. Section III is concerned with the semiclassical evaluation of the mapping formalism. After introducing the semiclassical propagator and its numerical implementation via an initial-value representation [39–44], the virtues and shortcomings of the semiclassical treatment of several mappings are investigated for a two-level system. It is shown that the mapping proposed in Ref. [24] appears to be the only transformation that provides an exact description of a general N-level system within a standard semiclassical evaluation. Adopting the well-known spin-boson model (i.e., a two-level system coupled to a single or many nuclear DoF), we furthermore present computational studies for this mapping. The performance of the semiclassical approximation in the case of regular and chaotic dynamics as well as for multimode relaxation dynamics is discussed in some detail. Section IV discusses the semiclassical description of nonadiabatic dynamics via spin-coherent states as well as its connection to the mapping procedure. Section V concludes.

II. MAPPING FORMALISM

There are a variety of formalisms that allow for a mapping of a discrete quantum system onto a continuous analog (for reviews, see Refs. [29,30]). The most prominent examples are Schwinger's theory of angular momentum [25] and the Holstein-Primakoff transformation [28]. In this section we briefly review both methods, and generalize the formulations to the representation of N-level systems.

A. Spin system

Let us consider a spin DoF, which is described by the spin operators S_1, S_2, and S_3, with commutation relations ($\hbar \equiv 1$)

$$[S_j,S_k]=i\epsilon_{jkl}S_l, \tag{2.1}$$

as well as the corresponding raising and lowering operators

$$S_\pm = S_1 \pm iS_2. \tag{2.2}$$

These operators act in the Hilbert space of spin states $|sm\rangle$ with

$$S_3|sm\rangle = m|sm\rangle, \quad -s\leqslant m\leqslant s, \quad s=\tfrac{1}{2},1,\tfrac{3}{2},\ldots. \tag{2.3}$$

Consider, furthermore, a $(2s+1)$-dimensional subspace of the Hilbert space with fixed s. Then, according to Schwinger's theory of angular momentum [25], this discrete spin DoF can be represented by two bosonic oscillators described by creation and annihilation operators $a_n^\dagger$ and a_m with commutation relations

$$[a_n,a_m^\dagger]=\delta_{n,m} \tag{2.4}$$

and basis states $|n_1,n_2\rangle$ which satisfy

$$a_1^\dagger a_1|n_1,n_2\rangle = n_1|n_1,n_2\rangle, \tag{2.5a}$$

$$a_2^\dagger a_2|n_1,n_2\rangle = n_2|n_1,n_2\rangle. \tag{2.5b}$$

The mapping relations read

$$S_+ \rightarrow a_2^\dagger a_1, \tag{2.6a}$$

$$S_- \rightarrow a_1^\dagger a_2, \tag{2.6b}$$

$$S_3 \rightarrow (a_2^\dagger a_2 - a_1^\dagger a_1)/2, \tag{2.6c}$$

$$|sm\rangle \rightarrow \frac{(a_1^\dagger)^{s-m}(a_2^\dagger)^{s+m}}{\sqrt{(s+m)!(s-m)!}}|0_1,0_2\rangle = |(s-m)_1,(s+m)_2\rangle. \tag{2.6d}$$

The idea of this transformation goes back to Jordan [45]. Therefore, it is sometimes called Jordan-Schwinger representation. The mapping preserves the commutation relations (2.1). As can be seen from Eq. (2.6d), the image of the $(2s+1)$-dimensional spin Hilbert space is the subspace of the two-oscillator Hilbert space with $2s$ quantum of excitation—the so-called physical subspace [29,46]. This subspace is invariant under the action of any operator which results by mapping (2.6) from an arbitrary spin operator $\mathcal{A}(S_1,S_2,S_3)$. Thus, starting in this subspace, the system will always remain in it. As a consequence, the mapping yields the following identity for the matrix-elements of an operator $\mathcal{A}$

$$\langle sm|\mathcal{A}|sm'\rangle = \langle (s-m)_1,(s+m)_2|A|(s-m')_1,(s+m')_2|\rangle, \tag{2.7}$$

where A denotes the transformed operator which results from $\mathcal{A}$ through the mapping relations (2.6). In particular, if $\mathcal{A}$ denotes the time-evolution operator of the spin system, we have the the following exact identity for the propagator:

$$\langle sm|e^{-i\mathcal{H}t}|sm'\rangle = \langle (s-m)_1,(s+m)_2|e^{-iHt}|(s-m')_1,(s+m')_2\rangle. \tag{2.8}$$

In the Schwinger representation the identity operator in the spin Hilbert space is mapped onto the constant of motion $a_1^\dagger a_1 + a_2^\dagger a_2$. The existence of this constant of motion is utilized by the Holstein-Primakoff transformation to eliminate one boson DoF, thus representing the spin DoF by a single oscillator [28]

$$S_+ \rightarrow \sqrt{2s}a^\dagger\sqrt{1-a^\dagger a/2s}, \tag{2.9a}$$

$$S_- \rightarrow \sqrt{2s}\sqrt{1-a^\dagger a/2s}a, \tag{2.9b}$$

$$S_3 \rightarrow a^\dagger a - s, \tag{2.9c}$$

$$|sm\rangle \rightarrow \frac{(a^\dagger)^{s+m}}{\sqrt{(s+m)!}}|0\rangle = |s+m\rangle. \tag{2.9d}$$

The Holstein-Primakoff transformation also preserves the commutation relation (2.1). Due to the square-root operators in Eqs. (2.9), however, the mutual adjointness of S_+ and S_- as well as the self-adjointness of S_3 is only guaranteed in the physical subspace $\{|0\rangle,\ldots,|s+m\rangle\}$ of the transformation [30]. This flaw of the Holstein-Primakoff transformation outside the physical subspace does not present a problem on the quantum-mechanical level of description. This is because the physical subspace again is invariant under the action of any operator which results from the mapping (2.9) of an arbitrary spin operator $\mathcal{A}(S_1,S_2,S_3)$. As discussed in Sec. III B, however, the square-root operators may cause serious problems in the semiclassical evaluation of the Holstein-Primakoff transformation.

Let us briefly mention some formal aspects of the above introduced formalism, which have been discussed in detail by Blaizot and Marshallek [29]. First, it is noted that both the Schwinger and Holstein-Primakoff representations are not

unitary transformations in the usual sense. Nevertheless, a transformation may be defined in terms of a formal mapping operator acting in the fermionic-bosonic product Hilbert space. Furthermore, the interrelation of the Schwinger representation and the Holstein-Primakoff representation has been investigated in the context of the quantization of time-dependent self-consistent fields. It has been shown that the representations are related to each other by a nonunitary transformation. This lack of unitarity is a consequence of the nonexistence of a unitary polar decomposition of the creation and annihilation operators a_n and $a_n^\dagger$ [47] and the resulting difficulties in the definition of a proper phase operator in quantum optics [48].

Finally, it is noted that there exist alternative mappings of spin to continuous DoF. For example, Ref. [30] discusses various mappings which (like the Holstein-Primakoff transformation) represent a spin system by a single boson DoF. The possibility of utilizing spin-coherent states for this purpose is discussed in Sec. IV.

B. *N*-level system

Let us now consider an N-level system with basis states $|\psi_n\rangle$ $(n=1,\ldots,N)$ and the Hamiltonian

$$\mathcal{H}=\sum_{n,m} h_{nm}|\psi_n\rangle\langle\psi_m|. \tag{2.10}$$

In obvious analogy to Schwinger's theory of angular momentum, this N-level system can be represented by N oscillators, whereby the mapping relations for the operator and the basis states read [24]

$$|\psi_n\rangle\langle\psi_m|\rightarrow a_n^\dagger a_m, \tag{2.11a}$$

$$|\psi_n\rangle\rightarrow|0_1,\ldots,1_n,\ldots,0_N\rangle. \tag{2.11b}$$

Here a_n and $a_m^\dagger$ are the usual oscillator creation and annihilation operators with bosonic commutation relations (2.4), and $|0_1,\ldots,1_n,\ldots,0_N\rangle$ denotes a harmonic-oscillator eigenstate with a single quantum excitation in the mode n. According to Eq. (2.11a), the bosonic representation of Hamiltonian (2.10) is given by

$$H=\sum_{n,m} h_{nm}a_n^\dagger a_m, \tag{2.12}$$

and the mapping preserves the commutation relations of the operator basis

$$[\,|\psi_n\rangle\langle\psi_m|\,,|\psi_k\rangle\langle\psi_l|\,]=|\psi_n\rangle\langle\psi_l|\,\delta_{m,k}-|\psi_k\rangle\langle\psi_m|\,\delta_{l,n}. \tag{2.13}$$

The image of the N-level Hilbert space is the subspace of the N-oscillator Hilbert space with a single quantum excitation. Again, this (physical) subspace is invariant under the action of any operator which results by mapping (2.11a) from an arbitrary N-level system operator. As a consequence we obtain the propagator identity

$$\langle\psi_n|e^{-i\mathcal{H}t}|\psi_m\rangle=\langle 0_1,\ldots,1_n,\ldots,0_N| \times e^{-iHt}|0_1,\ldots,1_m,\ldots,0_N\rangle. \tag{2.14}$$

For a two-level system, mapping (2.11) obviously coincides with Eq. (2.6) for $s=\frac{1}{2}$.

It is interesting to note that different bosonic Hamiltonians H may correspond to the same original Hamiltonian $\mathcal{H}$. This ambiguity reflects the fact that in the physical subspace an identity transformation of the bosonic Hamiltonian $H\rightarrow H'$ does not change the dynamics in this subspace. For example, the two bosonic Hamiltonians

$$H=E+V(a_1^\dagger a_2+a_2^\dagger a_1), \tag{2.15}$$

$$H'=E(a_1^\dagger a_1+a_2^\dagger a_2)+V(a_1^\dagger a_2+a_2^\dagger a_1) \tag{2.16}$$

are equivalent in the physical subspace $\{|0_1,1_2\rangle,|1_1,0_2\rangle\}$, and correspond to the same ''discrete'' two-level system Hamiltonian

$$\mathcal{H}=E+V(|\psi_1\rangle\langle\psi_2|+|\psi_2\rangle\langle\psi_1|). \tag{2.17}$$

Since H and H' are equivalent in the physical subspace, both Hamiltonians generate the same quantum dynamics in this subspace. However, this is not necessarily true if approximations are employed in the evaluation of the dynamics. For example, adopting a semiclassical approximation, the quantum mechanically equivalent Hamiltonians H and H' may yield different results. Experience shows that it is useful first to transform the Hamiltonian on the quantum-mechanical level to the simplest possible form (which in the present case would be H), and then to apply the semiclassical approximation.

As discussed above for the case of spin systems, formalism (2.11) is not the only way to construct a mapping of an N-level system. First of all it is clear that one may again eliminate one boson DoF by exploiting the identity operator $\Sigma_n a_n^\dagger a_n$ as constant of motion. Furthermore, one may express the N^2-dimensional operator basis in terms of powers of the spin matrices S_1, S_2, and S_3. Employing the Holstein-Primakoff (or Schwinger) transformation, the entire N-level system can thus be represented by one (or two) oscillator(s). On a classical level, this strategy has been followed by Meyer and Miller in their spin matrix mapping method [15]. Unfortunately, the higher powers of the spin operators result in highly nonlinear equations of motion, which are unfavorable for a semiclassical treatment.

The continuous quantum system (2.12) obtained by the mapping procedure can also be considered as the result of a second-quantization procedure restricted to the one-particle space. Although this point of view may appear artificial (because we do not deal with many-particle theory), it nevertheless elucidates the concept underlying the mapping approach and is therefore briefly considered in the following.

One way to derive a second-quantization formalism that has been anticipated by Dirac [49] is to represent the time-dependent wave function pertaining to the N-level system (2.10) as

$$|\psi(t)\rangle=\sum_n c_n(t)|\psi_n\rangle, \tag{2.18}$$

where the complex coefficients c_n obey the time-dependent Schrödinger equation

$$i\dot{c}_n=\sum_m h_{nm}c_m. \tag{2.19}$$

Let us introduce the expectation value of the Hamiltonian $\mathcal{H}$,

$$\tilde{H}=\langle\psi(t)|\mathcal{H}|\psi(t)\rangle=\sum_{n,m} c_n^* c_m h_{nm}$$

$$=\tfrac{1}{2}\sum_{n,m}(X_nX_m+P_nP_m)h_{nm}, \tag{2.20}$$

where $c_n=(X_n+iP_n)/\sqrt{2}$, and we have assumed that $h_{nm}=h_{nm}^*$. As first pointed out by Dirac, Hamilton's equations for $\tilde{H}$ and the real variables X_n and P_n are completely equivalent to the equation of motion (2.19) for the complex coefficients c_n [49,50]. Equation (2.20) can therefore be interpreted as classical Hamiltonian function representing N coupled harmonic oscillators.

Following the basic concept of second quantization, that is, to quantize not only observables but also the state vector, the classical oscillators are subsequently interpreted as quantum oscillators. Replacing the amplitudes c_n^* and c_n by the creation and annihilation operators $a_n^\dagger$ and a_n, the procedure directly leads to the quantum-mechanical mapping Hamiltonian (2.12). We note in passing that in the above derivation we have used bosonic creation and annihilation operators, thus retaining Hamiltonian (2.12) and the basis state (2.11b) of the mapping representation. Being restricted to a single-particle space, however, the many-particle statistic does not matter, and one could also use fermionic operators, thus retaining the Hamiltonian (2.10) in the discrete representation.

It is interesting to note that the derivation of the classical Hamiltonian function in the classical electron-analog model [14] is virtually identical up to Eq. (2.20). As discussed in Sec. I, however, this formulation does not establish a *quantum-mechanical* equivalence of the N-level system (2.10) and the N-oscillator system [Eq. (2.12)]. As a consequence, the classical model Hamiltonian neglects the commutator $[a_n,a_n^\dagger]=1$, which results in the $-\frac{1}{2}\Sigma_n V_{nn}$ term in the quantum Hamiltonian [Eq. (3.32)] describing the zero-point energy excitation of the electronic oscillators [27]. In order to achieve meaningful semiclassical quantization conditions ''Langer-like modifications'' were subsequently invoked to the off-diagonal elements of the Hamiltonian function. While the origin as well as the value of these modifications are difficult to justify in the classical model (see the discussion in Refs. [51,52]), the zero-point energy term naturally arises in the quantum-mechanical derivation.

III. SEMICLASSICAL DESCRIPTION

The mapping procedure introduced above results in quantum-mechanical Hamiltonians with well-defined classical analogs, thus rendering the semiclassical evaluation a straightforward matter. Following a brief description of semiclassical methods used in this work, the virtues and shortcomings of the semiclassical treatment of several mappings are studied for the case of a two-level system. Employing Schwinger's formulation to the spin-boson model, we furthermore perform computational studies on the semiclassical description of nonadiabatic dynamics.

A. Semiclassical propagator

Let us consider an n-dimensional quantum system with Hamiltonian H, which is assumed to possess a well-defined classical analog. In order to obtain the semiclassical approximation to the transition amplitude $K_t(f|i)$ between the initial state $|i\rangle$ and the final state $|f\rangle$, the amplitude is expressed in terms of the coordinate-dependent propagator $K_t(\mathbf{x}'|\mathbf{x})$

$$K_t(f|i)\equiv\langle f|e^{-iHt}|i\rangle=\int d\mathbf{x}'\int d\mathbf{x}\langle f|\mathbf{x}'\rangle K_t(\mathbf{x}'|\mathbf{x})\langle\mathbf{x}|i\rangle, \tag{3.1}$$

which then is evaluated within the semiclassical Van Vleck–Gutzwiller approximation [1]

$$K_t^{\mathrm{VVG}}(\mathbf{x}'|\mathbf{x})=\sum_{\mathrm{traj}}\frac{e^{iS_{\mathbf{x}}-i\pi\nu/2}}{\sqrt{\det(2\pi i\partial\mathbf{x}'/\partial\mathbf{p})}}. \tag{3.2}$$

Here the sum runs over all trajectories that start from point $\mathbf{x}_0=\mathbf{x}$ at time 0 and end up at point $\mathbf{x}_t=\mathbf{x}'$ at time t, $S_{\mathbf{x}}$ is the classical action along such a trajectory, and the monodromy matrix elements $\partial\mathbf{x}'/\partial\mathbf{p}$ account for the dependency of the trajectory $\mathbf{x}_t$ with respect to its initial momentum $\mathbf{p}_0$. The Maslov-index ν counts the zeroes of the Van Vleck determinant. The evaluation of the semiclassical Van Vleck–Gutzwiller propagator [Eq. (3.2)] amounts to the solution of a boundary-value problem. That is, given a trajectory characterized by the position $\mathbf{x}(t)=\mathbf{x}_t$ and momentum $\mathbf{p}(t)=\mathbf{p}_t$, we need to find the roots of the equation $\mathbf{x}_t=\mathbf{x}_t(\mathbf{x}_0,\mathbf{p}_0)$. To circumvent this cumbersome root search, one may rewrite the propagator as an initial-value problem [39–44]. As a consequence, the semiclassical propagator is given as a phase-space integral over the initial conditions $\mathbf{x}_0$ and $\mathbf{p}_0$, which is amenable to a Monte Carlo evaluation. For this reason, semiclassical initial-value representations are regarded as keys to the application of semiclassical methods to multidimensional systems.

In this work, we use a Herman-Kluk-type representation of the propagator [40], which can be written as

$$K_t^{\mathrm{HK}}(\mathbf{x}'|\mathbf{x})=\int\frac{d\mathbf{x}_0d\mathbf{p}_0}{(2\pi)^n}C_{\mathbf{x}_t\mathbf{p}_t}e^{iS_{\mathbf{x}}}\langle\mathbf{x}'|\mathbf{x}_t\mathbf{p}_t\rangle\langle\mathbf{x}_0\mathbf{p}_0|\mathbf{x}\rangle. \tag{3.3}$$

Here the classical action is given as

$$S_{\mathbf{x}}=\int_0^t d\tau(\dot{\mathbf{x}}_\tau\mathbf{p}_\tau-H^{\mathrm{Cl}}), \tag{3.4}$$

and the dynamics of the trajectories $\mathbf{x}_t$ and $\mathbf{p}_t$ is governed by the classical Hamiltonian function H^{Cl}. Furthermore, we have introduced coherent states $|\mathbf{x}_t\mathbf{p}_t\rangle$, which in the position representation are given by Gaussian wave packets

$$\langle \mathbf{x}|\mathbf{x}_t\mathbf{p}_t\rangle = \left(\frac{\gamma}{\pi}\right)^{n/4} \exp\left\{-\frac{\gamma}{2}(\mathbf{x}-\mathbf{x}_t)^2 + i\mathbf{p}_t(\mathbf{x}-\mathbf{x}_t)\right\}. \tag{3.5}$$

Throughout this paper, we have chosen a width parameter of $\gamma=1$. The complex function $C_{\mathbf{x}_t\mathbf{p}_t}$ describes the spreading of the Gaussian wave packets during their propagation in an anharmonic potential [40]

$$C_{\mathbf{x}_t\mathbf{p}_t} = \sqrt{\det\left[\frac{1}{2}\left(\frac{\partial \mathbf{p}_t}{\partial \mathbf{p}_0} + \frac{\partial \mathbf{x}_t}{\partial \mathbf{x_0}} - \gamma i \frac{\partial \mathbf{x}_t}{\partial \mathbf{p}_0} + \frac{i}{\gamma}\frac{\partial \mathbf{p}_t}{\partial \mathbf{x}_0}\right)\right]}. \tag{3.6}$$

In what follows, it is advantageous to rewrite the Herman-Kluk propagator $K_t(\mathbf{x}'|\mathbf{x}) = \langle \mathbf{x}'|K_t|\mathbf{x}\rangle$ in the basis-free form

$$K_t^{\mathrm{HK}} = \int \frac{d^2\mathbf{z_0}}{\pi^n} |\mathbf{z}_t\rangle C_{\mathbf{z}_t} e^{iS_{\mathbf{z}}} \langle \mathbf{z_0}|. \tag{3.7}$$

Here the integration measure is given by

$$d^2\mathbf{z_0} = d(\mathrm{Re}\mathbf{z}_0)\, d(\mathrm{Im}\mathbf{z}_0) = d\mathbf{x}_0 d\mathbf{p}_0/2^n, \tag{3.8}$$

and we have used complex variables $\mathbf{z}=(z_1,\ldots,z_n)=(\mathbf{x}+i\mathbf{p})/\sqrt{2}$ and coherent states

$$|\mathbf{z}\rangle = \exp\left(-\sum_j |z_j|^2/2\right) \exp\left(\sum_j z_j a_j^\dagger\right)|\mathbf{0}\rangle = |\mathbf{xp}\rangle e^{i\mathbf{px}/2} \tag{3.9}$$

to simplify the notation. The function $C_{\mathbf{z}_t}$ is given by

$$C_{\mathbf{z}_t} = \sqrt{\det(\partial \mathbf{z}_t/\partial \mathbf{z}_0)} = C_{\mathbf{x}_t\mathbf{p}_t} \tag{3.10}$$

and $S_{\mathbf{z}}$ denotes the action

$$S_{\mathbf{z}} = \int_0^t d\tau \left(\frac{i}{2}(\mathbf{z}_\tau^* \dot{\mathbf{z}}_\tau - \dot{\mathbf{z}}_\tau^* \mathbf{z}_\tau) - H^{\mathrm{Cl}}\right). \tag{3.11}$$

This action coincides (besides a boundary-value term) with the action that appears in the coherent-state path integral, and is therefore reminiscent of the origin of the Herman-Kluk propagator [53]. It should be noted that representation (3.7) of the Herman-Kluk propagator is only valid for a width parameter $\gamma=1$. To account for arbitrary values of γ, the usual coherent states $|\mathbf{z}\rangle$ need to be replaced by squeezed states.

It is noted that there exist several choices for the classical Hamiltonian H^{Cl} which correspond to different operator orderings. One possibility, which is supported by the derivation of the Herman-Kluk propagator from the coherent-state path integral [53], is to use the coherent-state matrix element (or Q function)

$$H_N^{\mathrm{Cl}}(\mathbf{z}) = \langle \mathbf{z}|H|\mathbf{z}\rangle. \tag{3.12}$$

This choice corresponds to a normal ordering of the quantum Hamiltonian with respect to creation and annihilation operators. In this case it is appropriate to use a correction term in the action, i.e.,

$$S_{\mathbf{z}} \to S_{\mathbf{z}} + \frac{1}{2}\int_0^t d\tau \sum_j \frac{\partial^2 H_N^{\mathrm{Cl}}}{\partial z_j \partial z_j^*}, \tag{3.13}$$

to treat low-energy states correctly [54]. Another possibility is to use a symmetrically x-p-ordered Hamiltonian, i.e., the Wigner function

$$H_W^{\mathrm{Cl}}(\mathbf{x},\mathbf{p}) = \int d\mathbf{s}\, e^{i\mathbf{sp}} \langle \mathbf{x}-\mathbf{s}/2|H|\mathbf{x}+\mathbf{s}/2\rangle. \tag{3.14}$$

Both possibilities have been discussed within the Wentzel-Kramers-Brillouin theory [54,55] as well as in the context of semiclassical approximations to phase-space path integrals [56]. In the computational studies reported below we have employed the Wigner representation (3.14) of the Hamiltonian, which seemed to yield slightly better results. For simple analytically solvable problems such as the harmonic oscillator, both choices are obviously equivalent.

B. Two-level system

In order to compare semiclassical approximations obtained for various mappings introduced above, it is instructive to investigate the dynamics of a simple two-level system with electronic matrix elements $h_{nn}=E_n$ and $h_{nm}=V$ $(n,m=1,2,\ n\neq m)$. Let us first consider the Schwinger representation (2.11) of the Hamiltonian

$$H_S = \sum_{n=1,2} E_n a_n^\dagger a_n + V(a_1^\dagger a_2 + a_2^\dagger a_1). \tag{3.15}$$

Using the symmetrically ordered Wigner function (3.14), the classical Hamiltonian reads

$$\begin{aligned} H_S^{\mathrm{Cl}} &= \sum_{n=1,2} E_n (z_n^* z_n - \tfrac{1}{2}) + V(z_1^* z_2 + z_2^* z_1) \\ &= \sum_{n=1,2} E_n \tfrac{1}{2}(x_n^2 + p_n^2 - 1) + V(p_1 p_2 + x_1 x_2). \end{aligned} \tag{3.16}$$

The transition amplitude in the Schwinger representation is given as

$$K_t(1|2) \equiv \langle \Psi_1|e^{-i\mathcal{H}t}|\Psi_2\rangle = \langle 1_1, 0_2|e^{-iH_S t}|0_1, 1_2\rangle. \tag{3.17}$$

Employing the Herman-Kluk propagator (3.7), the semiclassical transition amplitude reads

$$\begin{aligned} K_t^{\mathrm{S}}(1|2) = \int \frac{d^2 z_{10}}{\pi} \int \frac{d^2 z_{20}}{\pi} &\langle 1_1 0_2|z_{1t}, z_{2t}\rangle \\ &\times C_{z_{1t}, z_{2t}} e^{iS_z} \langle z_{10}, z_{20}|0_1, 1_2\rangle. \end{aligned} \tag{3.18}$$

As is well known, the Van Vleck–Gutzwiller approximation is exact if the Hamiltonian is quadratic [1]. This is the case for the Schwinger representation as well as for its generalization to N-level systems (2.11).

The Holstein-Primakoff (HP) representation of the two-level system Hamiltonian is given by

$$H_{\mathrm{HP}}=E_1(1-a^\dagger a)+E_2 a^\dagger a+V(a^\dagger\sqrt{1-a^\dagger a}+\sqrt{1-a^\dagger a}\,a). \tag{3.19}$$

The semiclassical approximation for the transition amplitude reads

$$K_t(1|2)=\langle 0|e^{-iH_{\mathrm{HP}}t}|1\rangle=\int\frac{d^2z_0}{\pi}\langle 0|z_t\rangle C_{z_t}e^{iS_z}\langle z_0|1\rangle. \tag{3.20}$$

While the classical Hamiltonian (3.16) pertaining to the Schwinger representation is well defined, the choice of a classical Hamiltonian in the Holstein-Primakoff representation is quite ambiguous. This is because the square-root operator in Eq. (3.19) is only well defined in the physical subspace, but otherwise leads to an imaginary contribution to the Hamiltonian. The simplest choice for a classical representation of the square-root operator is to use the classical approximation for Wigner function of a function of an operator, i.e.,

$$(f(a^\dagger a))_W=f((a^\dagger a)_W). \tag{3.21}$$

This way we obtain the classical Hamiltonian

$$H_{\mathrm{HP}}^{\mathrm{Cla}}=E_1(\tfrac{3}{2}-z^*z)+E_2(z^*z-\tfrac{1}{2})+V(z^*+z)\sqrt{\tfrac{3}{2}-z^*z} \tag{3.22}$$

and the corresponding equation of motion

$$\dot{z}=-i\frac{\partial H_{\mathrm{HP}}^{\mathrm{Cla}}}{\partial z^*}. \tag{3.23}$$

Obviously, this Hamiltonian is only well defined if $z^*z<\frac{3}{2}$. In the computational evaluation we therefore have to restrict the sampling of initial values to this region and exclude trajectories which approach $z^*z=\frac{3}{2}$. The resulting sampling scheme may be viewed as a practical implementation of the restriction onto the physical subspace on the classical level.

Another classical Hamiltonian can be obtained in the following way. Representing the square-root operator $f(a^\dagger a)=\sqrt{1-a^\dagger a}$ through an expansion in terms of harmonic-oscillator eigenstates, the Wigner function of this operator is given by

$$(f(a^\dagger a))_W(z)=2e^{-2|z|^2}\sum_{m=0}^{\infty}(-1)^m\sqrt{1-m}L_m(4|z|^2), \tag{3.24}$$

where $L_m(x)$ denotes a Laguerre polynomial. Note that the real part of Eq. (3.24) is given by the term with $m=0$, while the rest of the sum ($m>1$) gives the imaginary part. Since the Hamiltonian has to be real valued, it appears to be sensible to take only the real part into account, thus yielding the classical Hamiltonian

$$H_{\mathrm{HP}}^{\mathrm{Clb}}=E_1(\tfrac{3}{2}-z^*z)+E_2(z^*z-\tfrac{1}{2})+4V(z^*+z)e^{-2|z|^2}. \tag{3.25}$$

It is noted that Eq. (3.25) can also be obtained by a quantum-mechanical transformation of the Hamilton operator according to

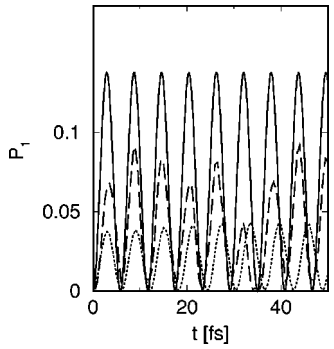

FIG. 1. Rabi oscillations of a two-level system. The full line represents the correct quantum result, while the broken lines correspond to results obtained by two variants of the semiclassical Holstein-Primakoff representation.

$$H_{\mathrm{HP}}\rightarrow H'_{\mathrm{HP}}=E_1(1-a^\dagger a)+E_2 a^\dagger a+V(|0\rangle\langle 1|+|1\rangle\langle 0|), \tag{3.26}$$

where $|0\rangle$ and $|1\rangle$ are the ground and first excited states of the oscillator. This transformation represents an identity in the physical subspace. The Wigner function of the operator H'_{HP} is then identical to Eq. (3.25). We note in passing that the interaction term $V(|0\rangle\langle 1|+|1\rangle\langle 0|)$ in H'_{HP} corresponds to the mapping

$$|\Psi_1\rangle\langle\Psi_1|\rightarrow|0\rangle\langle 0|, \tag{3.27a}$$

$$|\Psi_2\rangle\langle\Psi_2|\rightarrow|1\rangle\langle 1|, \tag{3.27b}$$

$$|\Psi_1\rangle\langle\Psi_2|\rightarrow|0\rangle\langle 1|, \tag{3.27c}$$

which was proposed by Garbaczewski [30] some time ago.

Let us illustrate these theoretical considerations by a representative computational example. Figure 1 shows the time-dependent population probability $P_1(t)=|K_t(1|2)|^2$ obtained for a two-level system with the parameters $E_2-E_1=0.658$ eV, and $V=0.132$ eV. Shown are the quantum result (full line) as well as the semiclassical results pertaining to the two variants of the semiclassical Holstein-Primakoff representation, $H_{\mathrm{HP}}^{\mathrm{Cla}}$ (dashed line) and $H_{\mathrm{HP}}^{\mathrm{Clb}}$ (dotted line). As discussed above, the semiclassical approximation to the two-level system is exact in the Schwinger representation, whereas the corresponding Holstein-Primakoff representation is not exact due to the higher powers of dynamical variables. In fact, both versions of the Holstein-Primakoff representation are found to yield rather poor results. While the first variant at least reproduces the correct frequency of the Rabi oscillations, the second variant is incorrect in both frequency and amplitude. As already mentioned, the reason for this failure lies in the complicated structure of the Hamiltonian which results in highly nonlinear equations of motion. The same problem occurs when higher powers of the spin operators S_1, S_2, and S_3 are used to represent a general N-level system ($N>2$). Although all these representations are exact on the quantum-mechanical level, the Schwinger representation as well as its generalization to N-level systems [Eq. (2.11)] are therefore clearly superior for a semiclassical evaluation.

C. Nonadiabatic dynamics

In the following we adopt the bosonic representation introduced in Eqs. (2.11) to describe nonadiabatic dynamics on coupled potential-energy surfaces. To this end, we identify the $|\psi_n\rangle$ with electronic states and the matrix elements h_{nm} of the Hamiltonian with operators of the nuclear dynamics. First numerical studies describing bound state [24] and reactive [26,57] nonadiabatic dynamics appeared to be quite promising. Here we wish to focus on specific problems associated with the semiclassical calculation of nonadiabatic dynamics. Employing a multidimensional molecular model, we furthermore present first results of a semiclassical description of nonadiabatic relaxation processes.

As is well known, a vibronic problem can be described in the adiabatic as well as diabatic electronic representations. The Hamiltonian matrix elements in the adiabatic representation read [58]

$$h_{nm}=(T(\mathbf{p})+W_n(\mathbf{x}))\delta_{n,m}-\Lambda_{nm}(\mathbf{x},p), \tag{3.28}$$

where W_n denotes the adiabatic Born-Oppenheimer potential-energy surfaces, T is the kinetic energy, and Λ represents the non-Born-Oppenheimer operator. In the diabatic representation we obtain

$$h_{nm}=(T(\mathbf{p})+V_0(\mathbf{x}))\delta_{n,m}+V_{nm}(\mathbf{x}), \tag{3.29}$$

where V_{nm} represent the elements of the diabatic potential matrix, and V_0 is a state-independent potential term. The adiabatic representation is unique, and is often advantageous for an interpretation of nonadiabatic relaxation processes. On the other hand, transitions between *diabatic* electronic states are important for an interpretation of spectroscopic data [59]. This is because in the vicinity of a surface crossing the electronic dipole transition operator is only smooth in the diabatic representation. For further information on general concepts of non-Born-Oppenheimer dynamics, see, for example, Refs. [58,59].

As is clear from the derivation above, the mapping can be employed to any electronic representation under consideration. Quantum mechanically, adiabatic and diabatic representations are related through a unitary transformation, and thus contain equivalent information. This is no longer true, however, once a classical approximation is made: Depending on whether the approximation is employed in the diabatic or in the adiabatic representation, the resulting classical Hamiltonian contains identical first-order nonadiabatic couplings but different second-order nonadiabatic couplings [60]. The reason for this ambiguity of the classical description is related to the general problem of classically vanishing commutators of quantum-mechanically noncommuting operators [61]. As already discussed above, characteristics of classical dynamics may therefore critically depend on the representation chosen. In particular, this choice may determine if the system shows regular or chaotic behavior, thus rendering the interpretation of (unique) quantum dynamics in terms of (ambiguous) classical dynamics a problem [62].

For the numerical studies discussed below, we consider a model of the spin-boson type [2], that is, an electronic two-state system with the diabatic matrix elements

$$T(\mathbf{p})+V_0(\mathbf{x})=\tfrac{1}{2}\sum_j \omega_j(p_j^2+x_j^2), \tag{3.30a}$$

$$V_{nn}(\mathbf{x})=E_n+\sum_j \kappa_j^{(n)}x_j+(\kappa_j^{(n)})^2/2\omega_j. \tag{3.30b}$$

Here x_j and p_j are the dimensionless position and momentum of the jth vibrational mode with the vibrational frequency ω_j and the state-dependent linear coordinate shift $\kappa_j^{(n)}/\omega_j$. E_n denotes the vertical transition energy of the diabatic state $|\psi_n\rangle$. The off-diagonal diabatic coupling $V_{12}=V_{21}$ is assumed to be constant. Introducing, furthermore, Cartesian electronic variables

$$X_n=(a_n^\dagger+a_n)/\sqrt{2}, \tag{3.31a}$$

$$P_n=i(a_n^\dagger-a_n)/\sqrt{2}, \tag{3.31b}$$

the molecular Hamiltonian in the diabatic bosonic representation finally reads

$$H=h_0(\mathbf{x},p)+\tfrac{1}{2}\sum_{n,m}(X_nX_m+P_nP_m)V_{nm}(\mathbf{x}), \tag{3.32a}$$

$$h_0(\mathbf{x},p)=T(\mathbf{p})+V_0(\mathbf{x})-\tfrac{1}{2}\sum_n V_{nn}(\mathbf{x}), \tag{3.32b}$$

where the nonlinearity of the spin-boson problem becomes evident in Eq. (3.32a). The mapping Hamiltonian (3.32) with matrix elements (3.30) represents the basis for the computational studies reported below.

To facilitate the discussion of computational results, let us introduce several time-dependent quantities that reflect the nonadiabatic dynamics under consideration. The semiclassical wave function for the nonadiabatic system (3.32) can be written as

$$\langle\mathbf{x}|\Psi(t)\rangle=\sum_n \Phi_n(\mathbf{x},t)|\psi_n\rangle, \tag{3.33a}$$

$$\Phi_n(\mathbf{x},t)=\int\frac{d\mathbf{X}_0d\mathbf{P}_0}{(2\pi)^N}\int\frac{d\mathbf{x}_0d\mathbf{p}_0}{(2\pi)^M}w_0C_{\mathbf{X}_t\mathbf{x}_t}e^{iS_{\mathbf{X}\mathbf{x}}}\langle\mathbf{x}|\mathbf{x}_t\mathbf{p}_t\rangle\chi_n(t), \tag{3.33b}$$

$$\chi_n(t)=\langle 1|X_{nt}P_{nt}\rangle\prod_{m\neq n}\langle 0|X_{mt}P_{mt}\rangle. \tag{3.33c}$$

Here $C_{\mathbf{X}_t\mathbf{x}_t}$ and $S_{\mathbf{X}\mathbf{x}}$ denote the Herman-Kluk determinant (3.6) and the classical action (3.4), respectively, incorporating both the electronic $\{X_n,P_n\}$ and nuclear $\{x_j,p_j\}$ DoF. The weight function w_0 accounts for the overlap of the multidimensional Gaussian at time $t=0$ with the initial vibronic wave function and $\langle k|X_{nt}P_{nt}\rangle$ denotes the projection of the electronic coherent state $|X_{nt}P_{nt}\rangle$ on the corresponding kth harmonic-oscillator eigenfunction. Furthermore we wish to introduce the autocorrelation function of the system,

$$J(t)=\langle\Psi(t)|\Psi(0)\rangle, \tag{3.34}$$

describing the overlap of the time-dependent wave function with its initial state. As is well known, the Fourier transform of $J(t)$ yields the electronic absorption spectrum. Moreover, the time evolution of the autocorrelation function can be used as a measure of the phase-space exploration of the system [63].

An important quantity in the discussion of nonadiabatic dynamics is the *total* time-dependent electronic population probability defined by

$$P_n(t)=\langle\Psi(t)|P_n|\Psi(t)\rangle, \tag{3.35}$$

where $P_n=|\psi_n\rangle\langle\psi_n|$ is the projection operator on the electronic state $|\psi_n\rangle$. Within the mapping formalism (2.11) there are several ways to define an electronic projection operator. Employing the bosonic representation of the state vector [Eq. (2.11b)], we obtain

$$P_n=|0_1,\ldots,1_n,\ldots,0_N\rangle\langle 0_1,\ldots,1_n,\ldots,0_N|, \tag{3.36}$$

thus resulting in a projection of the nth electronic DoF on the first excited harmonic-oscillator state, while all other electronic DoF's are projected on the harmonic-oscillator ground state. Alternatively, one may directly employ Eq. (2.11a), thus yielding

$$P_n=\tfrac{1}{2}(X_n^2+P_n^2-1). \tag{3.37}$$

Calculating the electronic population probability $P_n(t)$ through definition (3.37) again corresponds to a projection of the nth electronic DoF on the first excited harmonic-oscillator state, while the trace is taken over all other electronic DoF. Since quantum mechanically the dynamics of the electronic oscillators is restricted to single excitations, both electronic projectors are equivalent in a quantum-mechanical evaluation. In a semiclassical evaluation, however, this is only approximately true. In practice, nevertheless, both electronic projectors were found to lead to similar results. In the calculations reported below, definition (3.36) has been employed.

The computational methods employed can be summarized as follows. To calculate the semiclassical wave function, we have evaluated the phase-space integral in Eq. (3.33) via a standard Monte Carlo scheme. Hereby the initial conditions for both electronic and nuclear DoF are obtained through the sampling of the initial Gaussian overlap functions $\langle X_{n0}P_{n0}|0\rangle$ and $\langle x_{j0}p_{j0}|0\rangle$, respectively, $|0\rangle$ being the ground state of the harmonic oscillator. In order to improve the statistics of the Monte Carlo scheme, we have excluded strongly chaotic trajectories from the sampling. Following Kay [64], we have employed the modulus of the Herman-Kluk determinant (3.6) as a criterion of regularity of the dynamics and rejected all trajectories with $|C_t|>\epsilon$. To keep the number of rejected trajectories at less than 10%, we have used the values $\epsilon=100$ for Figs. 2 and 5, $\epsilon=50\,000$ for Figs. 3 and 6, and $\epsilon=2000$ for Figs. 4 and 7, respectively. To ensure convergence within this simple sampling scheme, 10^6 trajectories needed to be sampled. The equations of motion for the N electronic and M nuclear DoF as well as for the corresponding $2(N+M)\times 2(N+M)$ stability matrix were solved using a standard Runge-Kutta-Merson scheme. On a Silicon Graphics Origin 200, the computations typically required from one hour (for Fig. 1) up to one day (for Fig. 4) CPU time. The molecular parameters of the model systems under consideration are collected in Table I.

TABLE I. Molecular parameters of the model Hamiltonian (3.30) including vibrational frequencies ω, coordinate shifts κ, vertical electronic gaps E_2-E_1, and diabatic couplings V_{12}. For models I and II we have $\kappa^{(2)}=-\kappa^{(1)}=\kappa$, and for model III, $\kappa^{(2)}=\kappa$ and $\kappa^{(1)}=0$. All quantities are given in eV.

	ω	κ	E_2-E_1	V_{12}
Model I	0.066	0.066	0.658	0.132
Model II	0.066	0.099	0.0	0.066
Model III	0.07	0.09	0.91	0.06
	0.18	0.22		
	0.26	0.34		

To study the main features of the semiclassical evaluation of the mapping formalism, let us first consider the simple case of a weakly coupled spin-boson problem with a single vibrational mode, henceforth referred to as model I. The quantum and classical dynamics of one-mode spin-boson systems have been investigated by a number of workers employing a mixed quantum-classical description, i.e., without the inclusion of semiclassical phases [22,62]. The virtues and shortcomings of a true semiclassical description are illustrated in Fig. 2, which compares exact quantum results (full

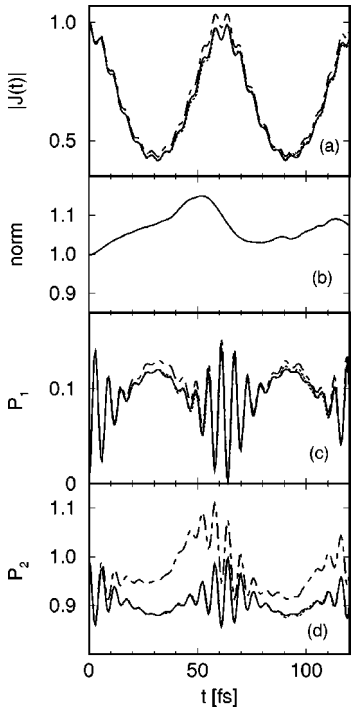

FIG. 2. Semiclassical description of the nonadiabatic dynamics exhibited by a one-mode spin-boson model (model I). Shown are exact quantum (full lines) and semiclassical (broken lines) results for (a) the modulus of the autocorrelation function $J(t)$, (b) the norm P_1+P_2 of the semiclassical wave function, and the electronic population probabilities (c) P_1 and (d) P_2. The dotted lines correspond to normalized semiclassical data, which are in excellent agreement with the quantum reference data.

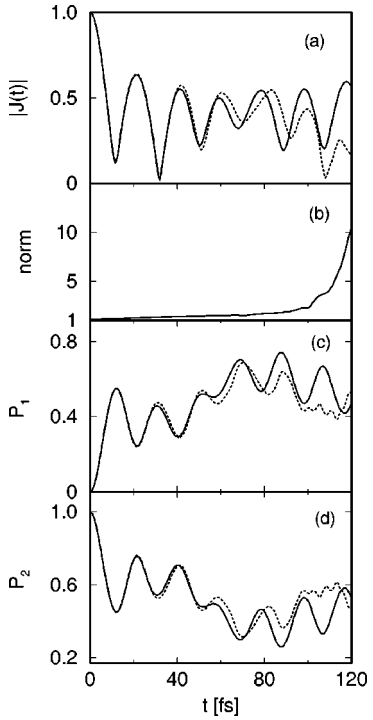

FIG. 3. The performance of the semiclassical mapping formulation for a highly chaotic system (model II). The semiclassical description (dotted lines) is able to match the exact quantum results (full lines) up to the time $t \approx 100$ fs. The labeling is the same as in Fig. 2.

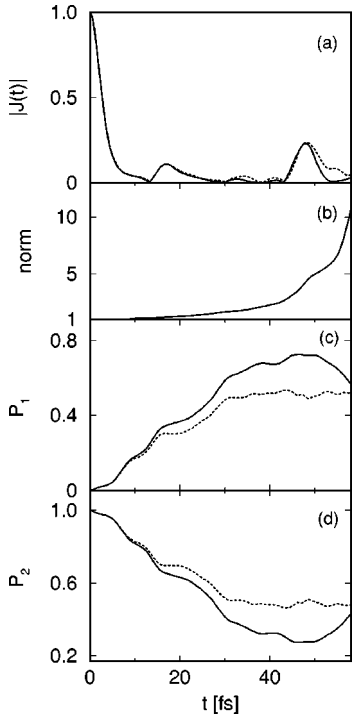

FIG. 4. Electronic relaxation dynamics exhibited by a three-mode spin-boson model (model III). The semiclassical results (dotted lines) qualitatively reproduce the exact quantum results (full lines) for the decay of the autocorrelation function and the excited-state population. The labeling is the same as in Fig. 2.

lines) to semiclassical results (broken lines) as obtained from Eq. (3.33). In all cases considered, we have assumed that the system is initially in the electronic state $|\psi_2\rangle$ and in the vibrational ground state of the unshifted harmonic oscillators. Shown are (a) the modulus of the autocorrelation function $J(t)$ defined in Eq. (3.34), the population probabilities (c) P_1 and (d) P_2 of the diabatic electronic states $|\psi_1\rangle$ and $|\psi_2\rangle$, respectively, and (b) the norm P_1+P_2 of the semiclassical wave function. The quantum results exhibit a high-frequency Rabi oscillation due to the electronic coupling which is superimposed by a low-frequency beating due to the vibrational motion. It is noted that electronic population probabilities $P_n(t)$ directly reflect the nonadiabatic dynamics of the system, i.e., in the absence of electronic coupling we have $P_1(t) \equiv 0$, $P_2(t) \equiv 1$.

Since the norm of the semiclassical wave function is only approximately conserved, the semiclassical results are displayed as rough data (dashed lines) and normalized data [e.g., $P_n^{\mathrm{N}} = P_n/(P_1+P_2)$, dotted lines]. The thus-obtained normalized results for the autocorrelation function and electronic population probabilities are seen to match the quantum reference data quantitatively. Employing a similar model, it was shown in Ref. [24] that the semiclassical wave function (3.33) maps the exact quantum-mechanical result in almost every detail. It is interesting to note that the deviation of the norm shown in Fig. 2(b) is not a numerical problem, but rather confirms the common wisdom that a two-level system as well as its bosonic representation is a prime example of a quantum system, and therefore difficult to describe within a semiclassical theory. Nevertheless, besides the well-known problem of norm conservation, the semiclassical mapping approach clearly reproduces the nonadiabatic quantum dynamics of the system. For simplicity, in the following we will restrict the discussion to normalized quantities.

Model I corresponds to a molecular system whose underlying classical dynamics is mostly regular. Although there exist a small fraction of chaotic trajectories, studies of various classical Poincaré sections reveal that phase space is predominately ordered [65]. To illustrate the performance of the mapping approach in the chaotic regime, we have adopted a model termed model II, in which the trajectories fill the complete energetically accessible phase space [65]. Figure 3 shows that the irregular classical dynamics is reflected in a complex structure of the time-dependent quantities. Furthermore, the semiclassical results are seen to deviate from the quantum data after several recurrences. Since the number of trajectories required to converge the phase-space integral in Eq. (3.33) increases exponentially in time, it is clear that in practice the semiclassical description of irregular dynamics is restricted to short times. Recently, several sophisticated strategies have been proposed to overcome this problem [66–68]. Here we just wish to conclude that—apart from generic problems associated with irregular dynamics—the semiclassical mapping approach is able to account for nonadiabatic quantum dynamics in the chaotic regime.

To demonstrate the capability of the approach, let us finally consider a multidimensional model problem. As discussed in detail in Ref. [59], a molecular system comprising two coupled electronic states and (at least) three vibrational modes may give rise to irreversible relaxation behavior of the electronic and vibrational dynamics. Here we adopt a three-mode model that was discussed by Wolfseder and

Domcke in the context of photoinduced electron-transfer processes [69]. Figure 4 demonstrates that the autocorrelation function and the excited-state population probability exhibit irregular structures and decay on different time scales, respectively. For larger times (not shown in Fig. 4), both quantities fluctuate around their long-time limits, thus clearly showing the irreversible relaxation behavior of a strongly-coupled few-mode system [59]. This vibronic relaxation dynamics is reflected in complex classical motion with mixed regular and irregular phase-space structures [70], thus rendering the semiclassical description a challenging problem. Figure 4 reveals that the semiclassical mapping approach qualitatively accounts for the decay of the autocorrelation function and the electronic population. For times $\gtrsim 40$ fs, the rapid increase of the norm indicates that the simple Monte Carlo sampling employed is no longer sufficient to converge the phase-space integral in Eq. (3.33).

IV. SPIN COHERENT STATES

The mapping approach relates a quantum system with discrete DoF to a system with continuous DoF which is amenable to a semiclassical treatment. Another possibility to obtain a continuous description of discrete DoF is based on the coherent states of the particular system under investigation [33,34]. This approach is well known for spin systems [36,71], but can also be applied to N-level systems. A general semiclassical formulation based on a stationary-phase approximation of the coherent-state path integral is given in Ref. [35]. Here we pursue a different route to a semiclassical spin-coherent-states description, and exploit the connection between spin-coherent states and Schwinger's representation of the corresponding spin system [72–74]. Employing the Herman-Kluk propagator (3.3) for a nonadiabatically coupled two-state system, we derive a new semiclassical initial-value representation for the corresponding spin-coherent-state propagator and apply the formulation to various models of nonadiabatic dynamics.

A. Notation

Let us start with a brief review of spin-coherent-state theory. For simplicity we focus on a two-level (or spin $\frac{1}{2}$) system, and leave the discussion of the more general N-level system to a separate article [65]. The coherent states for a two-level system with basis states $|\psi_1\rangle$ and $|\psi_2\rangle$ can be written as [37,71]

$$|\mu\rangle = \frac{\mu}{\sqrt{1+|\mu|^2}}|\psi_1\rangle + \frac{1}{\sqrt{1+|\mu|^2}}|\psi_2\rangle, \tag{4.1}$$

where μ is a complex parameter. As with the coherent states of the harmonic oscillator, these states are nonorthogonal,

$$\langle\mu|\mu'\rangle = \frac{1+\mu^*\mu'}{\sqrt{1+|\mu|^2}\sqrt{1+|\mu'|^2}}, \tag{4.2}$$

and overcomplete,

$$\mathbf{1} = \frac{2}{\pi}\int \frac{d^2\mu}{(1+|\mu|^2)^2}|\mu\rangle\langle\mu|. \tag{4.3}$$

Here the integration is over the complex plane,

$$d^2\mu = d(\mathrm{Re}\,\mu)\,d(\mathrm{Im}\,\mu). \tag{4.4}$$

Sometimes it is useful to parametrize the complex parameter μ by polar and azimuthal angles θ and ϕ $(0\leqslant\theta\leqslant\pi, 0\leqslant\phi\leqslant 2\pi)$ [75]

$$\mu = e^{i\phi}\tan\left(\frac{\theta}{2}\right). \tag{4.5}$$

The semiclassical approximation for the transition amplitude

$$\langle\psi'|e^{-i\mathcal{H}t}|\psi\rangle = \left(\frac{2}{\pi}\right)^2 \int \frac{d^2\mu_f}{(1+|\mu_f|^2)^2}\int \frac{d^2\mu_i}{(1+|\mu_i|^2)^2}\langle\psi'|\mu_f\rangle \times\langle\mu_f|e^{-i\mathcal{H}t}|\mu_i\rangle\langle\mu_i|\psi\rangle \tag{4.6}$$

is given through the stationary-phase evaluation of the path integral for the coherent state propagator, which formally reads [37]

$$\langle\mu_f|e^{-i\mathcal{H}t}|\mu_i\rangle = \int_{\mu_i}^{\mu_f}\mathcal{D}\mu\, e^{iS_\mu}, \tag{4.7}$$

with the action

$$S_\mu = \int_0^t d\tau\left(\frac{i}{2}\frac{\dot\mu\mu^* - \mu\dot\mu^*}{1+|\mu|^2} - \langle\mu|\mathcal{H}|\mu\rangle\right). \tag{4.8}$$

Although action (4.8) is nonquadratic in μ and μ^*, the semiclassical approximation to the path integral (4.7) yields (up to a normalization factor) the exact quantum-mechanical result. As discussed by several workers [37,76], this result, somewhat surprising on first sight, relies on the linearity of Heisenberg's equation of motion for the spin operators.

In the light of this fact, generalized coherent-state theory appears as a promising alternative for a semiclassical treatment of discrete quantum systems. In its present form, however, the theory is not suited for a computational evaluation. First the regularization procedure used to eliminate the infinite normalization factor [37] hampers a numerical implementation. To facilitate the calculation of multidimensional problems, furthermore, the boundary-value problem associated with the semiclassical approximation for the spin-coherent-state path integral needs to be rewritten in terms of an initial-value problem. With this end in mind, an initial-value representation for the semiclassical spin-coherent-state propagator is derived below.

B. Semiclassical propagator

Within the theoretical framework of time-dependent Hartree-Fock theory, Suzuki proposed an initial-value representation for a spin-coherent-states propagator [38]. Adopting a two-level system with quantum Hamiltonian $\mathcal{H}$, this propagator reads

$$K_t^{\mathrm{SU}} = N_t\frac{2}{\pi}\int \frac{d^2\mu_0}{(1+|\mu_0|^2)^2}|\mu_t\rangle e^{iS_\mu}\langle\mu_0|, \tag{4.9}$$

where N_t is a time-dependent factor guaranteeing the preservation of the norm of the semiclassical propagator. The dynamics of the classical trajectories is determined by the equation of motion

$$\dot{\mu} = -i(1+|\mu|^2)^2 \frac{\partial \langle \mu|\mathcal{H}|\mu\rangle}{\partial \mu^*}. \tag{4.10}$$

For a two-level system (or, more generally, for spin systems with a Hamiltonian that depends linearly on the spin operators S_1, S_2, and S_3) Suzuki's propagator gives the exact quantum-mechanical result and the normalization factor $N_t = 1$. A comparison of Eq. (4.9) with Eq. (3.7) reveals that Suzuki's propagator for spin-coherent states resembles the propagator of Herman and Kluk [Eq. (3.7)] employing harmonic-oscillator coherent states. Missing the determinant factor C_{z_t}, Suzuki's expression resembles Heller's ''frozen Gaussian approximation'' [77], and is thus expected to only yield approximate results in the case of a general nonlinear Hamiltonian.

In order to derive a semiclassically exact initial-value representation for the spin-coherent-states propagator, we again consider an electronic two-level system (3.32) coupled to M nuclear DoF. Introducing complex notations for an electronic DoF $\mathbf{Z}=(Z_1,Z_2)$ and a nuclear DoF $\mathbf{z}=(z_1,\ldots,z_M)$, the classical bosonic Hamiltonian [Eq. (3.32)] reads

$$H = h_0(\mathbf{z}) + \sum_{n,m=1}^{2} Z_n^* Z_m V_{nm}(\mathbf{z}), \tag{4.11}$$

and the equations of motion are given by

$$\dot{Z}_j = -i\frac{\partial H}{\partial Z_j^*}, \quad \dot{z}_j = -i\frac{\partial H}{\partial z_j^*}. \tag{4.12}$$

The Herman-Kluk propagator [Eq. (3.7)] pertaining to system (4.11), can be written as

$$\langle \psi'|K_t^{\mathrm{HK}}|\psi\rangle = \langle n_1',n_2'|e^{-iHt}|n_1,n_2\rangle = \int \frac{d^2\mathbf{z_0}}{\pi^M}\int\frac{d^2Z_1}{\pi}\int\frac{d^2Z_2}{\pi}|\mathbf{z}_t\rangle\langle n_1',n_2'|Z_{1_t},Z_{2_t}\rangle C_{\mathbf{Z}_t\mathbf{z}_t} e^{iS_{\mathbf{Z},\mathbf{z}}}\langle Z_{1_0},Z_{2_0}|n_1,n_2\rangle\langle \mathbf{z}_0|, \tag{4.13}$$

where $|\psi\rangle$ and $|\psi'\rangle$ denote the initial and final electronic states under consideration. Note that because of the mapping relation (2.11b), the quantum numbers in Eq. (4.13) fulfill the identity $n_1'+n_2'=1=n_1+n_2$.

In order to express propagator (4.13) in terms of spin-coherent states, we introduce the following parametrizations of the complex electronic variables [72]:

$$Z_{1_t} = \sqrt{I_t}\sin\left(\frac{\theta_t}{2}\right)e^{i(\phi_t-\psi_t)/2}, \tag{4.14a}$$

$$Z_{2_t} = \sqrt{I_t}\cos\left(\frac{\theta_t}{2}\right)e^{-i(\phi_t+\psi_t)/2}. \tag{4.14b}$$

Using Eq. (4.12), we obtain the equations of motion for the new electronic variables:

$$\dot{I} = 0, \tag{4.15a}$$

$$\dot{\psi} = V_{11}+V_{22}+2V_{12}\frac{\cos(\phi)}{\sin(\theta)}, \tag{4.15b}$$

$$\dot{\phi} = V_{22}-V_{11}-2V_{12}\cot(\theta)\cos(\phi), \tag{4.15c}$$

$$\dot{\theta} = -2V_{12}\sin(\phi). \tag{4.15d}$$

Due to the change of variables in Eq. (4.14), two of these equations of motion can readily be solved: The electronic population $I=|Z_1|^2+|Z_2|^2$ is a constant of motion, and Eq. (4.15b) can formally be integrated to give

$$\psi_t = \int_0^t ds\left\{V_{11}+V_{22}+2V_{12}\frac{\cos(\phi)}{\sin(\theta)}\right\}+\psi_0. \tag{4.16}$$

Note that the nuclear DoF $\mathbf{z}$ as well as the determinant factor $C_{\mathbf{z}_t\mathbf{z}_t}$ do not depend on ψ_0. Because the equations of motion for ϕ,θ and the nuclear DoF are independent of ψ, moreover, the electronic variables have a simple dependence on the initial phase ψ_0, (i.e., $Z_{1_t},Z_{2_t}\sim e^{-i\psi_0/2}$), thus allowing us to carry out the integration over ψ_0 in the semiclassical propagator. Expressing the electronic DoF in Eq. (4.13) in terms of the new variables (4.14), and employing the complex notation introduced in Eq. (4.5), the Herman-Kluk propagator can be written in the following form:

$$K_t^{\mathrm{HK}} = \int_0^\infty dI\frac{I^2}{2}e^{-I}\int\frac{d^2\mathbf{z_0}}{\pi^M}\frac{2}{\pi}\int\frac{d^2\mu_0}{(1+|\mu_0|^2)^2}|\mathbf{z}_t\rangle|\mu_t\rangle C_{\mathbf{Z}_t\mathbf{z}_t}\exp\{-i(1-I)(\psi_t-\psi_0+\phi_t-\phi_0)/2\}e^{iS_{\mu,\mathbf{z}}^I}\langle\mu_0|\langle\mathbf{z}_0|, \tag{4.17}$$

where the action is given by

$$S^I_{\mu,\mathbf{z}} = \int_0^t d\tau \left[\frac{i}{2}(\mathbf{z}_\tau^* \dot{\mathbf{z}}_\tau - \dot{\mathbf{z}}_\tau^* \mathbf{z}_\tau) - h_0(\mathbf{z}) \right] + I \int_0^t d\tau \left[\frac{i}{2}(\mu_\tau^* \dot{\mu}_\tau - \dot{\mu}_\tau^* \mu_\tau) - h_{\mathrm{el}}(\mathbf{z},\mu) \right], \tag{4.18}$$

and

$$h_{\mathrm{el}} = \frac{V_{22} + V_{11}\mu^*\mu + V_{21}\mu + V_{12}\mu^*}{1+\mu^*\mu} \tag{4.19}$$

denotes the part of the Hamiltonian which involves electronic variables. The derivation of Eq. (4.17) shows explicitly that only three electronic variables $(\theta_t, \phi_t, \psi_t)$ are time dependent and thus need to be propagated (and sampled at $t=0$), while the implementation of Eq. (3.18) requires the propagation of four variables (X_{1_t}, P_{1_t}, X_{2_t}, and P_{2_t}).

Up to now the Herman-Kluk propagator (3.7) has merely been rewritten without any further approximations. A comparison reveals, however, that the form of the propagator (4.17) is already very similar to Suzuki's expression (4.9). The most essential difference between the two formulations is the sampling over the initial value of the electronic population I in the Schwinger representation which is absent in Suzuki's propagator. Replacing the sampling by a fixed value $I=1$ (which corresponds to the quantum-mechanical value of the electronic population), we obtain

$$K_t^{\mathrm{SC}} = \frac{2}{\pi} \int \frac{d^2\mathbf{z_0}}{\pi^M} \int \frac{\mathrm{d}^2\mu_0}{(1+|\mu_0|^2)^2} |\mathbf{z}_t\rangle|\mu_t\rangle C_{\mathbf{z}_t\mathbf{z}_t} e^{iS_{\mu,\mathbf{z}}} \langle\mu_0|\langle\mathbf{z}_0|, \tag{4.20}$$

where the action $S_{\mu,\mathbf{z}}$ is given by Eq. (4.18), with $I=1$. Approximating the Herman-Kluk determinant factor $C_{\mathbf{z}_t\mathbf{z}_t}$ by the normalization factor N_t, the spin-coherent-state propagator (4.20) reduces to Suzuki's expression (4.9).

The semiclassical spin-coherent-state initial-value representations (4.17) and (4.20) are a central result of this paper. The derivation outlined above elucidates the close connection of Schwinger's representation and spin-coherent-state theory. Furthermore, various levels of approximation to the semiclassical spin-coherent-state propagator have been discussed: (i) the semiclassically exact propagator (4.17), (ii) the spin-coherent-state propagator (4.20) obtained from Eq. (4.17) by approximating the sampling over the electronic population I by its quantum value $I=1$, and (iii) Suzuki's propagator (4.9) obtained from Eq. (4.20) by replacing the determinant $C_{\mathbf{z}_t\mathbf{z}_t}$ by the normalization factor N_t. While for a simple two-level system all three descriptions are exact, their performances differ considerably in the general case of a nonlinear Hamiltonian (see below). Finally it should be stressed that—similarly to the Holstein-Primakoff representation (3.20)—the spin-coherent-state propagator (4.20) requires the sampling of only two (two instead of four) electronic variables [78]. Unlike the Holstein-Primakoff representation, however, the latter propagator is exact for a two-level system, and is found to yield much better results for general nonadiabatic problems.

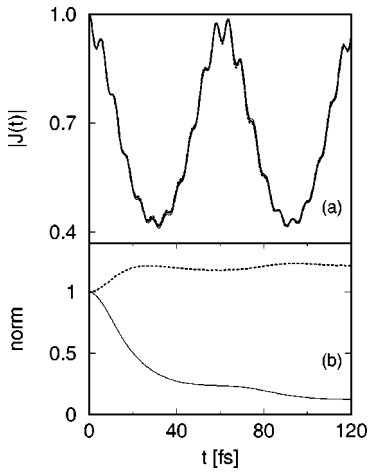

FIG. 5. (a) Modulus of the autocorrelation function $J(t)$ for model I as obtained by an exact quantum calculation (full line) and by a semiclassical evaluation employing the spin-coherent-state propagator (dotted line) and Suzuki's propagator (thin line). (b) Norm of the semiclassical wave function pertaining to the two semiclassical formulations.

C. Nonadiabatic dynamics

In what follows, we again adopt the model problems introduced in Sec. III C, and investigate the computational performance and accuracy of the spin-coherent-state propagator (4.20) and Suzuki's propagator (4.9). For brevity, and since the quality of the approximation is quite similar for the time-dependent quantities studied above, we focus on the discussion of the autocorrelation function.

Let us first consider model I, which represents a relatively weakly coupled one-mode spin-boson problem that exhibits predominantly regular classical dynamics. Figure 5 compares exact quantum (full line) and semiclassical (broken lines) results, thus demonstrating that for this relatively simple example both the spin-coherent-state propagator (4.20) and Suzuki's propagator (4.9) are in excellent agreement with the quantum reference. The main difference between the two semiclassical approximations is found in the norm of the semiclassical wave function shown in Fig. 5(b). While the determinant factor of the spin-coherent-state propagator preserves the norm fairly well, the norm of Suzuki's propagator is seen to decrease rapidly.

Comparing Figs. 5 and 2, it is interesting to note that the more approximate spin-coherent-state propagator (4.20) in fact yields slightly better results than the propagator (4.17), including the sampling of the electronic population I. This curiosity is related to the fact that trajectories with $I=1$ are typically more regular than trajectories with higher values of I. As a consequence, no trajectories were rejected in the sampling of the phase-space integral in Eq. (4.20), whereas in the numerical implementation of the initial-value representation (4.17) strongly chaotic trajectories needed to be excluded (cf. the discussion in Sec. III C). A closer analysis reveals that these rejected trajectories typically have large values of the electronic population I, and therefore do not occur in the semiclassical spin-coherent-state propagator.

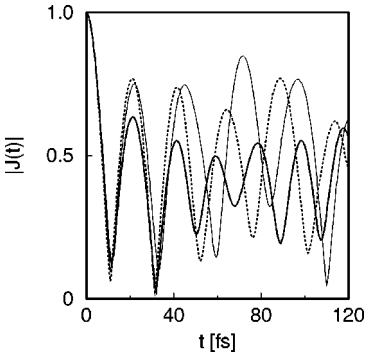

FIG. 6. Quantum and semiclassical spin-coherent-state results for the autocorrelation function of model II.

The situation is quite different for model II which represents a strongly coupled one-mode spin-boson problem that exhibits predominantly chaotic classical dynamics. Figure 6 demonstrates that both spin-coherent-state propagators produce much poorer results than the semiclassical propagator based on Schwinger's representation shown in Fig. 3. Obviously, the sampling of the electronic population is important to account for the underlying chaotic dynamics of the system.

As a last example, Fig. 7 shows the autocorrelation function for model III which represents a strongly coupled three-mode system that exhibits ultrafast electronic relaxation dynamics. This quite challenging problem clearly illustrates the quality of the three semiclassical approximations under consideration. While the results obtained by semiclassically exact propagator is in very good agreement with the quantum results (see Fig. 4) and the spin-coherent-state propagator yields a qualitative agreement, the results obtained by Suzuki's propagator are totally unreliable.

In conclusion, it has been shown that the spin-coherent-state propagator (4.20) represents a valuable formulation for the semiclassical description of nonadiabatic dynamics. In the case of predominantly chaotic classical dynamics, the performance of this propagator has been found to be inferior compared to the semiclassical propagator (4.17) based on Schwinger's representation. Since its numerical implementation is advantageous, the spin-coherent-state propagator nevertheless represents a promising approach to the semiclassical description of large molecular systems with many DoF.

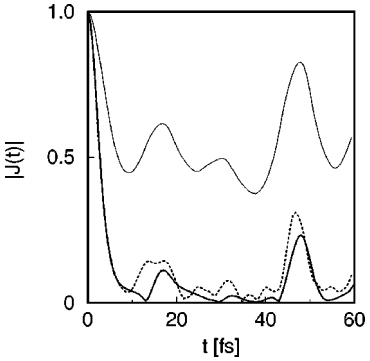

FIG. 7. Quantum and semiclassical spin-coherent-state results for the autocorrelation function of model III.

V. CONCLUSIONS

The mapping approach to the semiclassical description of nonadiabatic quantum dynamics consists of (i) an exact quantum-mechanical transformation of discrete quantum DoF onto continuous DoF, and (ii) a standard semiclassical treatment of the resulting dynamical problem. Since apart from the basic semiclassical Van Vleck–Gutzwiller approximation, no further assumptions or approximations are involved, the approach appears to be appealing both from a conceptional and a computational point of view.

We have discussed various possibilities to obtain a mapping from discrete to continuous DoF, in particular the Holstein-Primakoff transformation, Schwinger's transformation, and the spin-coherent-state representation. Although all these representations are exact on a quantum-mechanical level, the accuracy of their semiclassical evaluation has been shown to differ considerably. In particular, it has been shown that the generalization of Schwinger's theory proposed in Ref. [24] appears to be the only transformation that provides an exact description of a general N-level system within a standard semiclassical evaluation. On the other hand, it has been found that highly nonlinear terms in the mapping Hamiltonian (arising, e.g., in the Holstein-Primakoff transformation) hamper a successful semiclassical evaluation.

Apart from the choice of the quantum-mechanical mapping, there are several possibilities to establish a classical Hamiltonian function from the quantum Hamiltonian. For example, the semiclassical approximation depends on the choice of the representation (e.g., diabatic [Eq. (3.29)] or adiabatic [Eq. (3.28)]), as well as on the operator ordering (e.g., normal ordering [Eq. (3.12)] or symmetric ordering [Eq. (3.14)]) of the Hamiltonian. While this represents a general and well-known question, the semiclassical evaluation of the mapping formulation involves the additional problem that quantum-mechanical identity transformations within the physical subspace may lead to different classical expressions. This issue has been discussed in the context of the choice of the classical Hamiltonian [Eqs. (2.15) or (2.16)] as well as of electronic projectors [Eqs. (3.36) or (3.37)].

Exploiting the relation between spin-coherent states and Schwinger's representation for a two-state system, we have derived a semiclassical initial-value representation of the corresponding spin-coherent-state propagator. Several levels of approximation have been discussed: (i) the semiclassically exact propagator (4.17), (ii) the spin-coherent-state propagator (4.20) obtained from Eq. (4.17) by approximating the sampling over the electronic population I by its quantum value $I=1$, and (iii) Suzuki's propagator (4.9) obtained from Eq. (4.20) by replacing the determinant $C_{\mathbf{Z}_t\mathbf{z}_t}$ by the normalization factor N_t. Although the spin-coherent-state propagator (4.20) represents an approximation, the appealing numerical features of this propagator makes it a promising candidate for the semiclassical description of large molecular systems with many DoF.

Several continuations of this work appear promising. In the context of quantum signatures of irregular classical motion, it would be interesting to explore which classical mapping Hamiltonian results in the correct quantum-mechanical level statistic. First studies employing classical Poincaré sections have show that the order of phase space may signifi-

cantly depend on the particular bosonization chosen [65]. Furthermore, the semiclassical spin-coherent-state formulation can be extended in several ways, for example, to account for the dynamics of N-level systems. Finally, in order to push the limits of the semiclassical approach to the description of truly multidimensional dynamics, one needs to employ improved strategies to converge the phase-space integrations underlying the semiclassical initial-value representation. Examples include quasirandom sampling within the Sobol algorithm [79] and several integral conditioning methods [66–68]. Furthermore, suitable approximations to the semiclassically exact propagator such as the spin-coherent-state propagator (4.20) appear to be a promising way to the semiclassical description of complex systems.

ACKNOWLEDGMENTS

We thank Uwe Müller and Frank Grossmann for stimulating and helpful discussions and Peter Hänggi for critically reading the manuscript. M.T. furthermore thanks Wolfgang Domcke for his continuous encouragement. This work was supported by the Deutsche Forschungsgemeinschaft.

[1] M. C. Gutzwiller, *Chaos in Classical and Quantum Mechanics* (Springer, New York, 1990).
[2] U. Weiss, *Quantum Dissipative Systems* (World Scientific, Singapore, 1993).
[3] P. Pechukas, Phys. Rev. **181**, 174 (1969).
[4] W. H. Miller and T. F. George, J. Chem. Phys. **56**, 5637 (1972).
[5] D. F. Coker, in *Computer Simulation in Chemical Physics*, edited by M. P. Allen and D. J. Tildesley (Kluwer, Dordrecht, 1993), p. 315.
[6] E. C. G. Stückelberg, Helv. Phys. Acta **5**, 369 (1932).
[7] E. E. Nikitin, *Theory of Elementary Atomic and Molecular Processes in Gases* (Clarendon, Oxford, 1974).
[8] M. F. Herman, J. Chem. Phys. **81**, 754 (1984); **81**, 764 (1984); **103**, 8081 (1995).
[9] F. J. Webster, P. J. Rossky, and R. A. Friesner, Comput. Phys. Commun. **63**, 494 (1991).
[10] C. Zhu and H. Nakamura, J. Chem. Phys. **106**, 2599 (1997).
[11] J. C. Tully and R. K. Preston, J. Chem. Phys. **55**, 562 (1971); J. C. Tully, *ibid.* **93**, 1061 (1990).
[12] W. H. Miller and C. W. McCurdy, J. Chem. Phys. **69**, 5163 (1978).
[13] C. W. McCurdy, H.-D. Meyer, and W. H. Miller, J. Chem. Phys. **70**, 3177 (1979).
[14] H.-D. Meyer and W. H. Miller, J. Chem. Phys. **70**, 3214 (1979).
[15] H.-D. Meyer and W. H. Miller, J. Chem. Phys. **71**, 2156 (1979).
[16] H.-D. Meyer and W. H. Miller, J. Chem. Phys. **72**, 2272 (1980).
[17] R. Currier and M. F. Herman, J. Chem. Phys. **82**, 4509 (1985).
[18] N. F. Mott, Proc. Cambridge Philos. Soc. **27**, 553 (1931).
[19] J. B. Delos and W. R. Thorson, Phys. Rev. A **6**, 728 (1972).
[20] G. D. Billing, Chem. Phys. Lett. **30**, 391 (1975).
[21] R. B. Gerber, V. Buch, and M. A. Ratner, J. Chem. Phys. **77**, 3022 (1982).
[22] G. Stock, J. Chem. Phys. **103**, 1561 (1995).
[23] W. H. Miller, Adv. Chem. Phys. **25**, 69 (1974).
[24] G. Stock and M. Thoss, Phys. Rev. Lett. **78**, 578 (1997).
[25] J. Schwinger, in *Quantum Theory of Angular Momentum*, edited by L. C. Biedenharn and H. V. Dam (Academic, New York, 1965).
[26] X. Sun and W. H. Miller, J. Chem. Phys. **106**, 6346 (1997).
[27] U. Müller and G. Stock, J. Chem. Phys. **108**, 7516 (1998).
[28] T. Holstein and H. Primakoff, Phys. Rev. **58**, 1098 (1940).
[29] J. P. Blaizot and E. R. Marshalek, Nucl. Phys. A **309**, 422 (1978); **309**, 453 (1978).
[30] P. Garbaczewski, Phys. Rep. **36**, 65 (1978).
[31] A. Auerbach, *Interacting Electrons and Quantum Magnetism* (Springer, New York, 1994).
[32] M. S. Abdalla, S. S. Hassan, and A.-S. F. Obada, Phys. Rev. A **34**, 4869 (1986).
[33] J. R. Klauder and B.-S. Skagerstam, *Coherent States* (World Scientific, Singapore, 1985).
[34] A. M. Perelomov, *Generalized Coherent States and Their Applications* (Springer, Berlin, 1986).
[35] W.-M. Zhang and D. H. Feng, Phys. Rep. **252**, 1 (1995).
[36] J. R. Klauder, Phys. Rev. D **19**, 2349 (1979).
[37] E. Ercolessi, G. Morandi, F. Napoli, and P. Pieri, J. Math. Phys. **37**, 535 (1996).
[38] T. Suzuki, Nucl. Phys. A **398**, 557 (1983).
[39] W. H. Miller, J. Chem. Phys. **53**, 3578 (1970); **95**, 9428 (1991).
[40] M. F. Herman and E. Kluk, Chem. Phys. **91**, 27 (1984); M. F. Herman, Annu. Rev. Phys. Chem. **45**, 83 (1994).
[41] E. J. Heller, J. Chem. Phys. **94**, 2723 (1991).
[42] G. Campolieti and P. Brumer, J. Chem. Phys. **96**, 5969 (1992); Phys. Rev. A **50**, 997 (1994).
[43] K. G. Kay, J. Chem. Phys. **100**, 4377 (1994).
[44] M. A. Sepúlveda and F. Grossmann, Adv. Chem. Phys. **96**, 191 (1996).
[45] P. Jordan, Z. Phys. **94**, 531 (1935).
[46] J. P. Blaizot and G. Ripka, *Quantum Theory of Finite Systems* (MIT Press, Cambridge, 1986).
[47] L. Susskind and J. Glogower, Physics (Long Island City, NY) **1**, 49 (1964); P. Carruthers and M. N. Nieto, Rev. Mod. Phys. **40**, 411 (1968).
[48] See, for example, A. Luis and L. L. Sánchez-Soto, Phys. Rev. A **48**, 752 (1993).
[49] P. A. M. Dirac, Proc. R. Soc. London, Ser. A **114**, 243 (1927). See also W. Greiner, *Quantum Mechanics: Special Chapters* (Springer, Berlin, 1998), Chap. 3.
[50] F. Strocchi, Rev. Mod. Phys. **38**, 36 (1966).
[51] M. F. Herman and R. Currier, Chem. Phys. Lett. **114**, 411 (1985).
[52] G. Stock, J. Chem. Phys. **103**, 2888 (1995).
[53] F. Grossmann and A. L. Xavier, Jr., Phys. Lett. A **243**, 243 (1998).
[54] A. Voros, Phys. Rev. A **40**, 6814 (1989).

[55] J. Kurchan, P. Leboeuf, and M. Saraceno, Phys. Rev. A **40**, 6800 (1989).
[56] M. M. Mizrahi, J. Math. Phys. **22**, 102 (1981).
[57] V. S. Batista and W. H. Miller, J. Chem. Phys. **108**, 498 (1998).
[58] H. Köppel, W. Domcke, and L. S. Cederbaum, Adv. Chem. Phys. **57**, 59 (1984).
[59] W. Domcke and G. Stock, Adv. Chem. Phys. **100**, 1 (1997).
[60] U. Müller and G. Stock, J. Chem. Phys. **107**, 6230 (1997).
[61] A. Anderson, Ann. Phys. (N.Y.) **232**, 292 (1994).
[62] R. Graham and M. Höhnerbach, Z. Phys. B **57**, 233 (1984); L. Müller, J. Stolze, H. Leschke, and P. Nagel, Phys. Rev. A **44**, 1022 (1991); H. Schanz and B. Esser, *ibid.* **55**, 3375 (1997); R. Steib, J. L. Schoendorff, H. J. Korsch, and P. Reineker, J. Lumin. **76**, 530 (1998).
[63] E. J. Heller, Phys. Rev. A **35**, 1360 (1987).
[64] K. G. Kay, J. Chem. Phys. **101**, 2250 (1994).
[65] M. Thoss and G. Stock (unpublished).
[66] A. R. Walton and D. E. Manolopoulos, Mol. Phys. **87**, 961 (1996).
[67] B. W. Spath and W. H. Miller, J. Chem. Phys. **104**, 95 (1996).
[68] B. E. Guerin and M. F. Herman, Chem. Phys. Lett. **286**, 361 (1998).
[69] B. Wolfseder and W. Domcke, Chem. Phys. Lett. **259**, 113 (1996).
[70] D. M. Leitner, H. Köppel, and L. S. Cederbaum, J. Chem. Phys. **104**, 434 (1996).
[71] J. M. Radcliffe, J. Phys. A **4**, 313 (1971).
[72] Y. Takahashi and F. Shibata, J. Phys. Soc. Jpn. **38**, 656 (1975).
[73] M. Bergeron, Fortschr. Phys. **40**, 119 (1992).
[74] T. Boudjedaa *et al.*, J. Math. Phys. **36**, 1602 (1995).
[75] Some authors have employed a slightly different definition of spin-coherent states for $s=\frac{1}{2}$, i.e., $|\theta,\phi\rangle = e^{-i\phi S_3}e^{-i\theta S_2}|s,m=s\rangle = e^{-i\phi/2}|\mu\rangle$, which differs by a phase factor from the definition in Eq. (4.1).
[76] E. Keski-Vakkuri, A. J. Niemi, G. Semenoff, and O. Tirkkonen, Phys. Rev. D **44**, 3899 (1991); T. Fukui, J. Math. Phys. **34**, 4455 (1993); K. Funahashi, T. Kashiwa, S. Sakoda, and K. Fuji, *ibid.* **36**, 3232 (1995).
[77] E. J. Heller, J. Chem. Phys. **75**, 2923 (1981).
[78] The evaluation of the determinant factor $C_{\mathbf{Z}_t\mathbf{z}_t}$, however, seems to involve all four electronic variables. Rewriting the monodromy matrix $\partial(\mathbf{Z}_t\mathbf{z}_t)/\partial(\mathbf{Z}_0\mathbf{z}_0)$ in terms of the real electronic variables (4.14), it can be shown that the dimension of the monodromy matrix can be reduced from $(M+2)^2$ to $(M+1)^2$ [65].
[79] W. H. Press, S. A. Teukolsky, W. T. Vetterling, and B. P. Flannery, *Numerical Recipes*, 2nd ed. (Cambridge University Press, Cambridge, 1992).